Complex interplay of nonlinear processes in dielectric elastomers

Matthias Kollosche,[1,*] Jian Zhu,[2,*] Zhigang Suo,[2] and Guggi Kofod[1,†]

[1]*ACMP, Institut für Physik und Astronomie, Universität Potsdam, Karl-Liebknecht-Strasse 24-25, 14476 Potsdam, Germany*

[2]*School of Engineering and Applied Sciences, Kavli Institute of Bionano Science and Technology, Harvard University, Cambridge, Massachusetts 02138, USA*

A combination of experiment and theory shows that dielectric elastomers exhibit complex interplay of nonlinear processes. Membranes of a dielectric elastomer are prepared in various states of prestretches by using rigid clamps and mechanical forces. Upon actuation by voltage, some membranes form wrinkles followed by snap-through instability, others form wrinkles without the snap-through instability, and still others fail by local instability without forming wrinkles. Membranes surviving these nonlinear processes are found to attain a constant dielectric strength, independent of the state of prestretches. Giant voltage-induced stretch of 3.6 is attained.

PACS number(s): 82.35.Lr, 61.41.+e, 77.84.Jd

I. INTRODUCTION

An elastomeric membrane can be readily stretched to many times its initial area by mechanical forces, but inducing such a large deformation by voltage is difficult. An important discovery was made about a decade ago that voltage-induced deformation can be greatly enhanced by prestretch [1,2], which also increases the apparent electric breakdown field more than ten times [3,4]. The discovery has led to hundreds of designs of musclelike actuators, sensors, and generators, with promising applications such as soft robots, artificial limbs, adaptive optics, Braille displays, and energy harvesting [5,6].

The discovery has also led to intense studies of the physics of dielectric elastomers [6,7]. When a membrane of a dielectric elastomer is subject to voltage, the thickness decreases and the electric field increases. This positive feedback can drastically amplify the electric field and thin down the elastomer, leading to electromechanical instability (EMI) [8,9]. The EMI should be differentiated from another process: electric breakdown (EB), in which the intense electric field causes a path of conduction in a dielectric. Theory shows that the EMI can sometimes be removed by prestretches [10,11]. The EMI is also removed when a corona is used to spray charge on a dielectric elastomer without electrodes [12,13]. The EMI can even be harnessed to achieve giant voltage-induced deformation [14,15], form patterns [16,17], and mimic coexistent phases [10,18].

While these advances are intriguing, the physical mechanism by which the prestretch increases the apparent electric breakdown field remains unclear; hence, no method exists to predict achievable voltage-induced deformation. The lack of fundamental understanding limits applications that require long-term reliability and complex maneuvers, such as in soft robots and energy harvesting. This paper studies the increase in breakdown field due to prestretch by introducing a relatively simple setup—a membrane prestretched using rigid clamps and a mechanical force. We find that the clamped membrane can achieve much larger voltage-induced deformation than an unclamped membrane. We show that this simple setup

of clamped membrane displays remarkably rich interplay of nonlinear processes, including processes which result from voltage rate and stretch and which amplify the electric field leading to local instability, wrinkling, and snap-through instability. We further show that membranes surviving these nonlinear processes attain a constant dielectric strength, independent of the state of prestretches. Our findings provide insight into a salient feature of dielectric elastomers: large voltage-induced deformation is intimately tied to various nonlinear processes. This insight will guide the creation of large-deformation transducers.

II. EXPERIMENTAL

Figure 1 illustrates the setup. A membrane of a dielectric elastomer is pulled horizontally, fixed to rigid clamps, and pulled vertically by a constant mechanical force P. The rigid clamps and the mechanical force prepare the membrane in a state of prestretches, $\{\lambda_{1p}, \lambda_{2p}\}$. Subsequently, voltage Φ is applied to actuate the membrane to stretches $\{\lambda_1, \lambda_2\}$. The voltage-induced stretch is defined by λ_1/λ_{1p}. Large voltage-induced deformations were previously observed in membranes mounted on rigid rings [1], or membranes prestretched in one direction [1], or membranes subject to biasing pressure [15]. These setups do not allow direct force coupling to the surroundings, precluding their use as actuators. The clamped membrane allows direct force coupling, and is still simple enough for analytical treatment. The clamped membrane also resembles many of the more elaborate dielectric elastomer transducers, such as spring-loaded rolls [3,19] and hinged actuators [20,21]. Full nonlinear processes and breakdown conditions, however, are unknown for any of these setups.

We find that clamped membranes can achieve giant voltage-induced deformation. A clamped membrane of prestretches $\{2,5\}$, for example, attains an actuation stretch of 3.6, which is the highest ever reported for a free-standing dielectric elastomer with direct force coupling. Our calculation shows that, during actuation, if the clamps are assumed to hold the horizontal stretch fixed, $\lambda_2 = \lambda_{2p}$, the EMI is absent. The experiment, however, shows that the clamps do not always hold the horizontal stretch fixed. As the voltage increases, the horizontal tensile stress decreases and can even vanish. Upon loss of tension, the membranes form wrinkles. Some of

---

*These authors contributed equally to the paper.
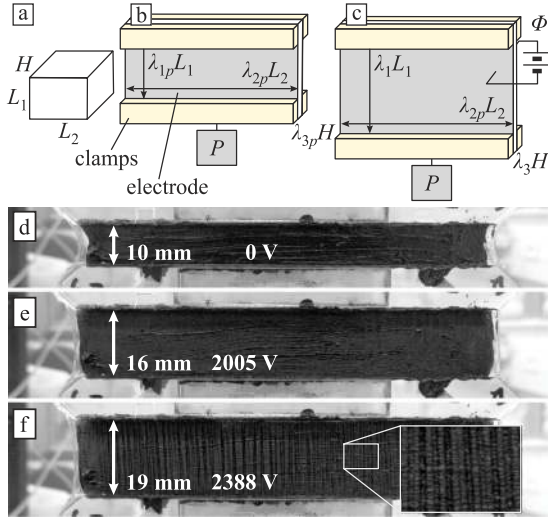
†Corresponding author: guggi.kofod@alumni.uni-potsdam.de

FIG. 1. (Color online) (a) In the reference state, under no force and voltage, the elastomer is of dimensions L_1, L_2, and H. (b) In the prestretched state, the elastomer is stretched horizontally, fixed to rigid clamps, and subjected to constant force P in the vertical direction. The dimensions of the elastomer become $\lambda_{1p}L_1$, $\lambda_{2p}L_2$, and $\lambda_{3p}H$. (c) In the actuated state, subject to both the force P and voltage Φ, the dimensions of the elastomer become $\lambda_1 L_1$, $\lambda_2 L_2$, and $\lambda_3 H$. Photographs of an elastomer in (d) a prestretched state, (e) an actuated state at 2005 V, and (f) an actuated state at 2388 V. The faint horizontal lines in (d) and (e) are smear lines in the grease electrodes, which arise from the means of their application and have no influence on deformation of the elastomer.

the membranes then undergo global snap-through instability. When prestretches are small, however, the membranes fail by local instability without forming wrinkles.

Membranes of VHB4905, an acrylic elastomer produced by 3M, are prepared in various states of prestretches $\{\lambda_{1p},\lambda_{2p}\}$, and actuated by using a voltage amplifier at a ramp rate of 5 V/s (more details are available in the Supplemental Material [22]). The slow ramp rate minimizes the effect of viscoelasticity, and the high aspect ratio of the membrane minimizes the effect of edges. A membrane of prestretches $\{4,5\}$ is shown in Fig. 1. The vertical dimension of the membrane is 10 mm in the prestretched state, and becomes 16 mm in an actuated state of 2005 V, corresponding to a voltage-induced stretch of 1.6. The membrane is smooth in the prestretched state, and remains smooth when the voltage is below a critical value [Fig. 1(e)]. When the voltage exceeds the critical value, the membrane forms wrinkles [Fig. 1(f)], as was anticipated in a previous theoretical study [23]. The onset of the wrinkles is rapid, but their wavelength decreases gradually. Videos for actuating membranes of prestretches $\{2,5\}$ and $\{4,5\}$ are available online [22].

III. OBSERVATIONS

Figure 2 shows measured voltage-stretch curves. Each curve corresponds to a membrane prepared in a specific state of prestretches $\{\lambda_{1p},\lambda_{2p}\}$, actuated by the voltage amplifier. The curve terminates at failure, when the electric current exceeds a threshold (0.5 mA) that trips the amplifier. The membrane is typically destroyed by a spark and a pinhole, sometimes
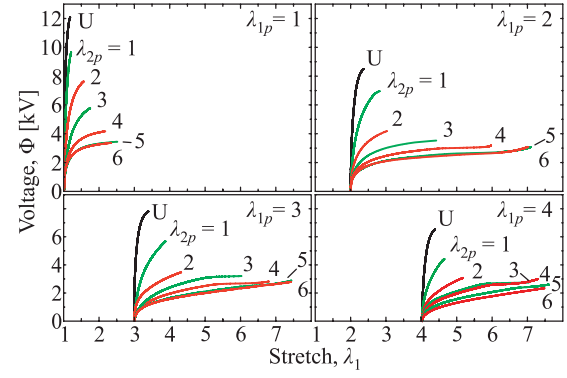

FIG. 2. (Color online) The experimentally recorded voltage-stretch curves for clamped membranes prepared in various states of prestretches $\{\lambda_{1p},\lambda_{2p}\}$. Also included are voltage-stretch curves for unclamped membranes, marked by "U".

followed by rupture. Included for comparison in Fig. 2 are the voltage-stretch curves for unclamped membranes. These curves, marked by "U," rise steeply. The voltage at failure decreases with increasing λ_{1p}. For $\lambda_{1p} = 2$, 3, and 4, the voltage-stretch curves become almost flat near failure, indicating the approach towards the snap-through instability. Actual snap-through instability, however, is not observed. Unclamped membranes attain rather small voltage-induced stretches, less than 1.3.

By contrast, many of the clamped membranes attain much larger voltage-induced stretches, and are actuated at lower voltages. For the membrane of prestretches $\{2,5\}$, the vertical stretch attains $\lambda_1 = 7.2$ before failure, corresponding to a voltage-induced stretch of $\lambda_1/\lambda_{1p} = 3.6$. All curves show an initial portion with negative curvatures. Some membranes fail on the initial portion (e.g., $\{2,1\}$). In many other cases, however, the stretches increase greatly within small changes in voltage. For example, for the membrane of prestretches $\{2,4\}$, the curve kinks at 2800 V, after which the curve is almost flat from stretch 4.6 to 5.5. In some cases, the jump is cut short by failure (e.g., $\{2,3\}$).

IV. THEORY

We next interpret the observed behavior by theoretical calculations. The elastomer is taken to be incompressible, $\lambda_1\lambda_2\lambda_3 = 1$, so that the elastic free energy per unit volume is a function of the in-plane stretches, $W(\lambda_1,\lambda_2)$. As the elastomer is stretched, the end-to-end distance of each polymer chain approaches its contour length, and the elastomer stiffens steeply. This strain-stiffening behavior is captured by the Gent model $W = -(\mu J_{\lim}/2)\ln[1 - (\lambda_1^2 + \lambda_2^2 + \lambda_3^2 - 3)/J_{\lim}]$, where μ is the shear modulus, and $J_{\lim}$ is a constant related to the limiting stretch [23,24]. The equations of state are $\sigma_1 + \varepsilon E^2 = \lambda_1 \partial W(\lambda_1,\lambda_2)/\partial\lambda_1$ and $\sigma_2 + \varepsilon E^2 = \lambda_2 \partial W(\lambda_1,\lambda_2)/\partial\lambda_2$, where $\sigma_1 = \lambda_1 P/(HL_2)$ is the stress in the vertical direction, σ_2 is the stress in the horizontal direction, $E = \lambda_1\lambda_2\Phi/H$ is the electric field, and ε is the permittivity. The parameters used in our calculations are $\mu = 30$ kPa, $J_{\lim} = 125$, and $\varepsilon = 4.65 \times 8.85 \times 10^{-12}$ F/m [3]. For an unclamped membrane, $\sigma_2 = 0$, and the equations of state are solved for λ_1 and λ_2. For a clamped membrane, λ_2 is prescribed by the prestretch λ_{2p},

and the equations of state are solved for λ_1 and σ_2. When a clamped membrane forms wrinkles, we set $\sigma_2 = 0$ and solve the equations of state for λ_1 and λ_2.

V. ANALYSIS OF ACTUATION CURVE SHAPE

Figure 3(a) shows the calculated voltage-stretch curves for unclamped membranes. The shapes of the curves are understood as follows [10]. At a small stretch, the voltage increases with the stretch. At an intermediate stretch, the thinning of the membrane amplifies the electric field, so that the voltage falls as the stretch increases. As the elastomer approaches the limiting stretch, the steep strain stiffening prevails, and the voltage rises again. In the experiment, the voltage is programmed to ramp up. When the voltage reaches the local maximum, the membrane suffers EMI, leading to EB. The local maximum of voltage corresponds to the state of the largest achievable deformation, so that the voltage-induced stretches of unclamped membranes are less than 1.3. This prediction is consistent with experimental observations shown in Fig. 2.

By contrast, Fig. 3(b) plots voltage-stretch curves for clamped membranes. When the clamps are assumed to hold the horizontal stretch fixed, $\lambda_2 = \lambda_{2p}$, the voltage-stretch curves are monotonic, indicating the absence of the EMI. The experimental observation of wrinkles, however, indicates that the clamps do not always hold the horizontal stretch fixed. Our calculation confirms that, as the voltage ramps up, the horizontal tensile stress decreases and eventually vanishes at a specific state of voltage and stretch, marked by an open circle. After the loss of tension, the membrane is in effect unclamped. For the membranes of prestretches {2,2}, {2,3}, and {2,4}, the loss of tension occurs as a local maximum of the voltage-stretch curve, Figs. 3(c)–3(e). For the membrane of prestretches {2,5}, however, the voltage-stretch curve is monotonic. These theoretical results correspond directly to the complex behavior observed in experiments.

VI. MODES OF FAILURE

We identify several modes of failure, marked by red crosses in Figs. 3(c)–3(f). In the first mode of failure, Fig. 3(c), a membrane fails prior to the global loss of tension. While the clamps hold horizontal stretch fixed at the top and bottom of the membrane, the clamps do not suppress inhomogeneous deformation in the interior of the membrane. Local instability occurs at a point in the membrane where the Hessian of the free energy function becomes singular. Following the method of [8], we calculate the determinant of the Hessian, and predict the state of local instability by setting the determinant to zero. Experiment shows that the membranes of small prestretches fail without forming wrinkles. All membranes with $\lambda_{1p} = 1$, as well as membranes of prestretches {2,1}, {2,2}, {3,1}, {3,2}, {4,1}, and {4,2}, fail by this local instability. A comparison between the experimental observation and theoretical prediction will be discussed later using Fig. 4.

In the second mode of failure, Fig. 3(d), a membrane survives the local instability, suffers the global loss of tension, followed by the snap-through instability. Experiment shows that the membrane forms wrinkles when the voltage exceeds a critical value, and fails during a sudden dramatic deformation. The voltage-stretch curve is nearly flat at the failure. Because the membrane fails during the snap before reaching the stable state, such behavior is unsuitable for application as actuators. The membranes of prestretches {2,3} and {3,3} exhibit this mode of failure.

In the third mode of failure, Fig. 3(e), a membrane survives the local instability, the global loss of tension, and the snap-through instability; the membrane only fails *after* it snaps and reaches the stable state. This theoretical prediction is also supported by experimental observations of wrinkles and sudden dramatic deformation. Remarkably, the experiment shows that the voltage-stretch curve kinks up with a positive curvature. Because the membrane fails after it snaps and reaches the stable state, the failure can be contained and the large stretch may be used in applications. Membranes of prestretches of {2,4}, {3,4}, {4,3}, and {4,4} exhibit this behavior.
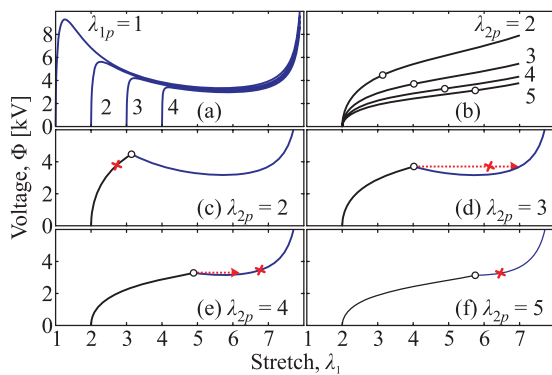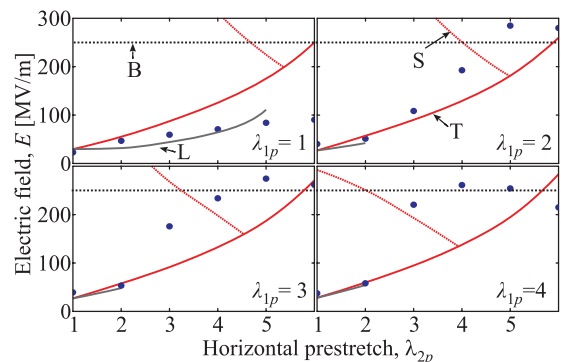

FIG. 3. (Color online) Theoretical predictions of voltage-stretch curves for (a) unclamped elastomer subject to constant uniaxial forces, and (b)–(f) clamped elastomer subject to a constant vertical force. (b) Calculation assumes that λ_2 is fixed, and the open circles signify the loss of horizontal tension. (c)–(f) Before loss of tension, λ_2 is fixed by the clamps. After loss of horizontal tension, the elastomer is in effect unclamped.

FIG. 4. (Color online) The apparent electric breakdown fields for membranes prepared in various states of prestretches {$\lambda_{1p}, \lambda_{2p}$}. The dots are experimental data. The lines correspond to intrinsic breakdown (B), loss of tension (T), stable states after the snap (S), and local instability (L).

In the fourth mode of failure, Fig. 3(f), the voltage-stretch starts with a negative curvature when the horizontal stretch is constrained by the clamps, and switches to a negative curvature upon loss of tension. The entire voltage-stretch curve, however, is monotonic. This theoretical prediction is supported by experimental observations of wrinkles and monotonic voltage-stretch curves. As shown in Fig. 2, the membranes of prestretches {2,5}, {2,6}, {3,5}, {3,6}, {4,5}, and {4,6} exhibit this behavior.

Figure 4 plots the apparent breakdown fields for membranes of various prestretches $\{\lambda_{1p}, \lambda_{2p}\}$. The dots are obtained from experimental data as follows. Each curve in Fig. 2 terminates in electric breakdown, where the voltage Φ and stretch λ_1 at failure are measured. Before loss of tension, $\lambda_2 = \lambda_{2p}$; after loss of tension, λ_2 is calculated theoretically by assuming $\sigma_2 = 0$, as explained above. The apparent breakdown field is calculated from $E = \Phi \lambda_1 \lambda_2 / H$.

Also plotted in Fig. 4 are curves of various theoretical predictions: local instability, loss of tension, and stable states after the snap. When prestretches are small, the observed apparent breakdown fields are close to those predicted by local instability. When prestretches are large, the observed apparent breakdown fields are nearly a constant, around 250 MV/m, independent of the state of prestretches. This behavior is reached by membranes of prestretches {2,5}, {2,6}, {3,4}, {3,5}, {3,6}, {4,3}, {4,4}, {4,5}, and {4,6}. As also shown in Fig. 2, all these membranes fail when voltage-stretch curves

kink up. This constant breakdown field appears to be a material parameter, as is likely to be the case for avalanche-type intrinsic breakdown [25].

VII. CONCLUSION

In summary, we have shown that a relatively simple setup—a clamped membrane of dielectric elastomer—displays remarkably rich interplay of nonlinear processes, including local instability, wrinkling, and snap-through instability. Giant voltage-induced stretch of 3.6 is achieved. Snap-through instability itself does not always lead to failure; under certain conditions a membrane can survive the snap and reach a stable state. Membranes surviving various nonlinear processes can attain a constant dielectric strength, independent of the state of prestretches. It is hoped that this understanding of the nonlinear processes and breakdown conditions will inform large-deformation applications such as soft robots and energy harvesting.

[1] R. Pelrine, R. Kornbluh, Q. B. Pei, and J. Joseph, Science **287**, 836 (2000).

[2] R. Pelrine, R. Kornbluh, and G. Kofod, Adv. Mater. **12**, 1223 (2000).

[3] G. Kofod, P. Sommer-Larsen, R. Kronbluh, and R. Pelrine, J. Intell. Mater. Syst. Struct. **14**, 787 (2003).

[4] J. S. Plante and S. Dubowsky, Int. J. Solids Struct. **43**, 7727 (2006).

[5] F. Carpi, S. Bauer, and D. De Rossi, Science **330**, 1759 (2010).

[6] P. Brochu and Q. B. Pei, Macromol. Rapid Commun. **31**, 10 (2010).

[7] Z. G. Suo, Acta Mechanica Solida Sinica **23**, 549 (2010).

[8] X. H. Zhao and Z. G. Suo, Appl. Phys. Lett. **91**, 061921 (2007).

[9] A. N. Norris, Appl. Phys. Lett. **92**, 026101 (2008).

[10] X. H. Zhao, W. Hong, and Z. G. Suo, Phys. Rev. B **76**, 134113 (2007).

[11] S. J. A. Koh, T. F. Li, J. X. Zhou, X. H. Zhao, W. Hong, J. Zhu, and Z. G. Suo, J. Polym. Sci., Part B: Polym. Phys. **49**, 504 (2011).

[12] C. Keplinger, M. Kaltenbrunner, N. Arnold, and S. Bauer, Proc. Natl. Acad. Sci. USA **107**, 4505 (2010).

[13] B. Li, J. X. Zhou, and H. L. Chen, Appl. Phys. Lett. **99**, 244101 (2011).

[14] X. H. Zhao and Z. G. Suo, Phys. Rev. Lett. **104**, 178302 (2010).

[15] C. Keplinger, T. F. Li, R. Baumgartner, Z. G. Suo, and S. Bauer, Soft Matter **8**, 285 (2012).

[16] Q. M. Wang, L. Zhang, and X. H. Zhao, Phys. Rev. Lett. **106**, 118301 (2011).

[17] Q. M. Wang, M. Tahir, L. Zhang, and X. H. Zhao, Soft Matter **7**, 6583 (2011).

[18] R. Huang and Z. G. Suo, Proc. R. Soc. A **468**, 1014 (2012).

[19] G. Kovacs, P. Lochmatter, and M. Wissler, Smart Mater. Struct. **16**, 306 (2007).

[20] P. Lochmatter and G. Kovacs, Sens. Actuators, A **141**, 577 (2008).

[21] C. Jordi, A. Schmidt, G. Kovacs, S. Michel, and P. Ermanni, Smart Mater. Struct. **20**, 075003 (2011).

[22] See Supplemental Material at http://link.aps.org/supplemental/10.1103/PhysRevE.85.051801 for description of the manufacture of samples and movies.

[23] D. Corbett and M. Warner, J. Phys. D: Appl. Phys. **42**, 115505 (2009).

[24] A. N. Gent, Rubber Chem. Technol. **69**, 59 (1996).

[25] L. A. Dissado and J. C. Fothergill, *Electrical Degradation and Breakdown in Polymers* (Peter Peregrinus Ltd, London, 1992).